ARTICLE

BIOTECHNOLOGY and BIOENGINEERING

Effects of Water Miscible Organic Solvents on the Activity and Conformation of the Baeyer–Villiger Monooxygenases From *Thermobifida fusca* and *Acinetobacter calcoaceticus*: A Comparative Study

Francesco Secundo,[1] Stefano Fialà,[1] Marco W. Fraaije,[2] Gonzalo de Gonzalo,[1] Massimiliano Meli,[1] Francesca Zambianchi,[1] Gianluca Ottolina[1]

[1]Istituto di Chimica del Riconoscimento Molecolare, CNR, via Mario Bianco 9, 20131 Milano, Italy; telephone: 39-02-285-000-29; fax: 39-02-285-000-36; e-mail: francesco.secundo@icrm.cnr.it

[2]Laboratory of Biochemistry, Groningen Biomolecular Sciences and Biotechnology Institute, University of Groningen, Groningen, The Netherlands

Received 12 April 2010; revision received 3 September 2010; accepted 16 September 2010

Published online 11 October 2010 in Wiley Online Library (wileyonlinelibrary.com). DOI 10.1002/bit.22963

ABSTRACT: A broader exploitation of enzymes in organic synthesis can be achieved by increasing their tolerance toward organic solvents. In this study, the stability and activity of Baeyer–Villiger monooxygenases from *Thermobifida fusca* (PAMO) and *Acinetobacter* sp. (CHMO) in the presence of water miscible organic solvents were compared. PAMO was more stable than CHMO. The concentration of solvent (v/v) at which it halved its activity (C_{50}) was 4- to 16-fold higher than that observed for CHMO. For PAMO, the C_{50} varied from 16% to 55% of solvent and followed the destabilizing order methanol < ethanol < 1,4-dioxane < acetonitrile < trifluoroethanol. In the case of CHMO, the maximal C_{50} was 7% with methanol and even lower with the other solvents. Therefore, methanol was the most tolerated solvent. In the case of PAMO, methanol induced a significant increase of enzyme activity (up to fivefold), which was optimal at 20% (v/v) solvent. Only minor spectral variations were observed with PAMO in 20% methanol, suggesting that the increase of activity observed in this condition is not due to marked conformational changes. Fluorescence and circular dichroism analyses showed that the lower stability of CHMO toward organic solvent correlates with a more pronounced destructive effect on its secondary and tertiary structure. A possible rationale for the higher stability of PAMO could be inferred from inspection of the PAMO and CHMO (two enzymes of similar size) structure, which revealed a higher (up to twofold) number of ionic bridges in PAMO with respect to CHMO.

Biotechnol. Bioeng. 2011;108: 491–499.

KEYWORDS: protein stability; fluorescence; circular dichroism; flavoenzyme; organic solvent; homology modelling

Correspondence to: F. Secundo

Additional Supporting Information may be found in the online version of this article.

Introduction

Biocatalysis is an approach commonly employed for the enantioselective synthesis of a large number of compounds of interest in the pharmaceutical, agricultural, and food industry (Woodley, 2008). Nevertheless, the application of enzymes for synthetic purposes is often hindered by the low solubility of many compounds in aqueous buffers, which causes a low performance of the biocatalyst. A strategy to overcome this limitation is the use of co-solvents (e.g., water miscible organic solvents) that increase the solubility of hydrophobic substrates in the reaction medium. However, organic solvents can affect activity, stability, and enantioselectivity of enzymes (Olofsson et al., 2005; Öztürk et al., 2010). In particular, they often impair enzymatic activity by altering the protein structure. Therefore, studies on the effects of organic solvents on protein conformation can enrich the knowledge base for addressing procedures useful to engineer robust enzymes suitable for biotechnological applications (e.g., biocatalysis in non-conventional media).

Among oxidoreductases, the Baeyer–Villiger monooxygenases (BVMOs) catalyze the oxidation of ketones to esters or cyclic ketons into lactones. Furthermore, they can stereoselectively oxygenate heteroatom-containing compounds (e.g., sulfoxidations, *N*-oxidations; Colonna et al., 1996; Ottolina et al., 1999). These enzymes are composed of a single polypeptide, contain FAD as a flavin cofactor and use NADPH as electron donor (Torres Pazmiño et al., 2010; Willetts, 1997). The catalytic mechanism involves the reaction of NADPH-reduced flavin with molecular oxygen to generate a stable flavin-peroxide intermediate that attacks

the carbonyl carbon of the substrate. Rearrangement of the resulting Criegee intermediate yields the oxygenated product and a hydroxy-flavin adduct, which is dehydrated to regenerate the oxidized flavin. Next, it follows the release of the product (ester) and of the NADP+ (Torres Pazmiño et al., 2008; Sheng et al., 2001).

Phenylacetone monoxygenase from *Thermobifida fusca* (PAMO; Fraaije et al., 2005) and cyclohexanone monoxygenase from *Acinetobacter calcoaceticus* (CHMO; Donoghue et al., 1976) are two BVMOs that have numerous biocatalytic applications (Alphand et al., 2003; Kamerbeek et al., 2003; Mihovilovic, 2006). The sequence identity between CHMO (543 amino acids) and PAMO (542 amino acids) is 40.3% (Bocola et al., 2005). PAMO is the most stable representative of this group of enzymes, being both thermally stable (at 52°C the enzyme showed a half-life of 24 h and was active up to 70°C) and stable toward organic solvents (De Gonzalo et al., 2006), which is very useful for application purposes. CHMO, which has a different substrate specificity compared to PAMO (Kayser, 2009), is less thermally stable than PAMO (CHMO halves its activity at 39°C) and low concentration of organic solvents lead to its rapid inactivation (Secundo et al., 2005).

In the present study, which was carried out in the context of our research on the use of monooxygenases for biocatalytic purposes, we focused on the effects of water-miscible protic and aprotic organic solvents on the activity and stability of PAMO and CHMO. The finding that a significant increase in activity of PAMO took place in the presence of 20% methanol (MeOH) prompted us to investigate by CD and fluorescence analyses, the influence of the solvent on enzyme conformation.

Materials and Methods

Materials

All chemicals and solvents were purchased from Sigma–Aldrich–Fluka and were of the highest quality grade available.

BVMOs

PAMO was obtained as previously described by Fraaije et al. (2005) and recombinant CHMO as reported by Secundo et al. (2005). Both enzymes were homogeneous as indicated by SDS–PAGE (data not shown). The specific activity of PAMO and CHMO was 0.09 and 3.0 (U/mg of protein), respectively. One unit of BVMO oxidizes 1.0 μmol of thioanisole to methyl phenyl sulfoxide per minute in 50 mM TRIS–HCl buffer, pH 8.6 and 25°C, in the presence of NADPH. The enzymatic activity was assayed at 25°C by monitoring NADPH consumption at 340 nm ($\varepsilon_{340} = 6.22$ mM/cm). Protein concentration assay was carried out by BIORAD reagent.

BVMOs Activity and Stability Measurements

The activity assay was carried out adding 0.1 mg of PAMO or 0.275 μg CHMO in air-saturated buffer containing the organic solvent from 0% to 60% (v/v), 1.0 mM of thioanisole, and 0.1 mM NADPH (final volume 1.0 mL).

The measurements of stability were performed incubating at 25°C PAMO or CHMO (1.0 U/mL) in the buffer containing the desired percentage of organic solvent. At different times, aliquots were withdrawn and the catalytic activity tested in the presence of the same organic solvent concentration as during pretreatment.

Fluorescence Measurements

Intrinsic fluorescence emission spectra of BVMOs were recorded over the 270–400 nm range with a Jasco FP-550 spectrofluorimeter equipped with a Peltier thermostat. An excitation wavelength of 295 nm was used to minimize the emission arising from tyrosine residues. Fluorescence of FAD was monitored by excitation at 440 nm and recording spectra from 400 to 600 nm. In all cases protein concentration was 0.02 mg/mL. The concentration of the standard *N*-acetyl-L-tryptophan ethyl ester (N-Ac-Trp-O-Et) was 0.01 mg/mL and that of FAD 0.002 mg/mL. All spectra were recorded at 25°C just after sample preparation. The effect of temperature on the fluorescence spectra of PAMO in the absence and in the presence of 20% MeOH was studied by recording spectra 1 min after the sample reached the desired temperature and exploring the temperature range with increments of 5°C.

Circular Dichroism Measurements

Far-UV circular dichroism (CD) spectra were recorded with a Jasco 600 spectropolarimeter over the 200–250 nm range, the optical path being 0.1 cm and the temperature 25°C. Enzyme concentration was 0.12 mg/mL. All the spectra were baseline corrected and smoothed by using the Spectra Analysis JASCO software.

Computational Analyses

The three-dimensional (3D) structural model of CHMO was generated by homology modeling on the basis of the crystal structures of cyclohexanone monooxygenase from *Rhodococcus* sp. strain HI-31 in the closed (PDB-code 3GWD) and in the open structure (PDB-code 3GWF; Mirza et al., 2009) using the program ICM-Homology and using default values (Abagyan and Totrov, 1994). The structures obtained from the homology modeling were energy minimized using Macromodel 9.7 (Schrodinger, LLC, New York). The energy minimization using the AMBER force field was done until gradient convergence (Weiner et al., 1984, 1986). The number of hydrogen bonds was calculated using Maestro package (Schrodinger, LLC).

Geometrical relations between four atoms, the donor hydrogen atom (H), the acceptor atom (A), the donor atom (D) bonded to H, and another neighbour atom (B) bonded to A, define hydrogen bonds. A hydrogen bond between H and A should meet the following criteria: (1) the distance is <2.50 Å, (2) the angle formed by D–H···A is >120°, (3) the angle formed by H···A–B is >90°. Salt bridges were determined using the VMD program (Humphrey et al., 1996), which allows the identification of a salt bridge if the distance between the oxygen atoms of acidic residues and the nitrogen atoms of basic residues are within the cut-off distance of 3.2 Å. The percentage of internal residues that are hydrophobic was calculated by identifying all the internal residues by the program GETAREA and counting the number of the hydrophobic residues. The PAMO structure used for the comparison with the homology model of CHMO was already in the PDB database (1W4X).

Results and Discussion

Activity and Stability of PAMO and CHMO in Water–Organic Solvent Mixtures

The effect of several water miscible organic solvents on the activity of PAMO and CHMO is shown in Figure 1. All the solvents tested caused, at high concentration, loss of enzyme activity, but no linear correlation was found between this phenomenon and several physical parameters of the organic solvents (Table I). Only with alcohols was it observed that C_{50} (the concentration of solvent in buffer at which half inactivation of the enzyme is observed) increased as a function of relative hydrophobicity (logP) and of pKa. For both enzymes methanol was the solvent most tolerated. Interestingly, the addition of methanol also resulted in a significant increase of activity in the case of PAMO (up to fivefold with 20% MeOH, as shown in Fig. 1). The increase in activity was only 1.2-fold for CHMO and maximal at 2% MeOH. It has to be noted that activation of enzymes at low co-solvent concentration, is a phenomenon already observed for other enzymes (Kudryashova et al., 2003; Ogino et al., 2000; Olofsson et al., 2006; Park et al., 2005; Tan and Lovrien, 1972). Interestingly, Tóth et al. (2010) found a remarkable increase in activity of the flavoenzyme NADH oxidase from *Thermus thermophilus* in the presence of several alcohols (with MeOH the optimum was at about 40%). For the rest of the organic solvents tested, PAMO seemed to tolerate them better than CHMO, especially when using EtOH. However, with these solvents no increase in the activity was observed.

Because of the favorable implications that the increase of enzyme activity can have in an industrial biocatalytic process, the stability of both enzymes in the presence of different percentages of MeOH and with thioanisole as model substrate was investigated (Fig. 2). PAMO in 20% MeOH preserves 93% of its initial activity after 24 h, which is similar to that of the control (96%). Instead, with 40% MeOH inactivation was much faster (Fig. 2b). CHMO showed very poor stability against MeOH and no activity was observed after 24 h in the presence of 5% MeOH (Fig. 2a).

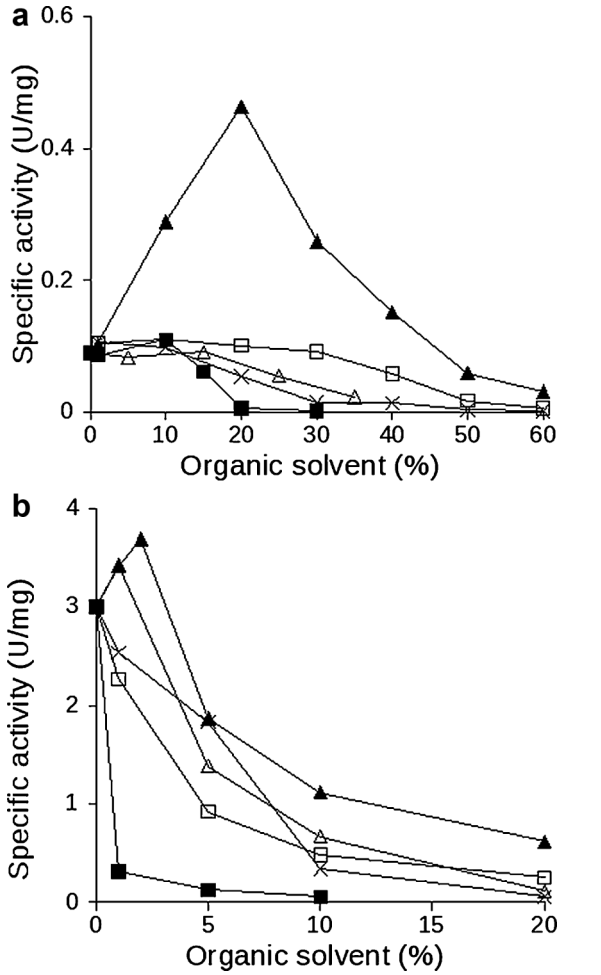

Figure 1. Specific activity of PAMO (**a**) and of CHMO (**b**) in water–organic solvent mixtures. The activity was measured just after adding the enzyme in the water–organic solvent mixture. Standard deviations were less than 10%. ACN (cross); MeOH (black triangle), EtOH (white square), TFE (black square), 1,4-dioxane (white triangle). See Materials and Methods Section for experimental details.

Table I. C_{50}[a] of BVMOs and characteristics of organic solvents.

Solvent	C_{50}PAMO	C_{50}CHMO	ε[b]	I[c]	pKa[d]	LogP[e]	DC[f]
MeOH	55	7	32.7	5.1	15.5	−0.8	30.5
EtOH	43	3	24.6	4.3	15.9	−0.2	54.4
1,4-Dioxane	26	5	2.2	4.8	—	−1.1	92.1
ACN	22	6	35.9	5.8	—	−0.3	64.3
TFE	16	1	26.7	—	12.4	0.4	—

[a] C_{50} (% v/v).
[b] Solvent dielectric constant at 25°C.
[c] Polarity index according to Gupta et al. (1997).
[d] Negative logarithm of acid dissociation constant (Riddick et al., 1986).
[e] Partitioning coefficient of the solvent in the water/1-octanol biphasic system (Leo et al., 1971).
[f] Denaturation capacity (Khmelnitsky et al., 1991).

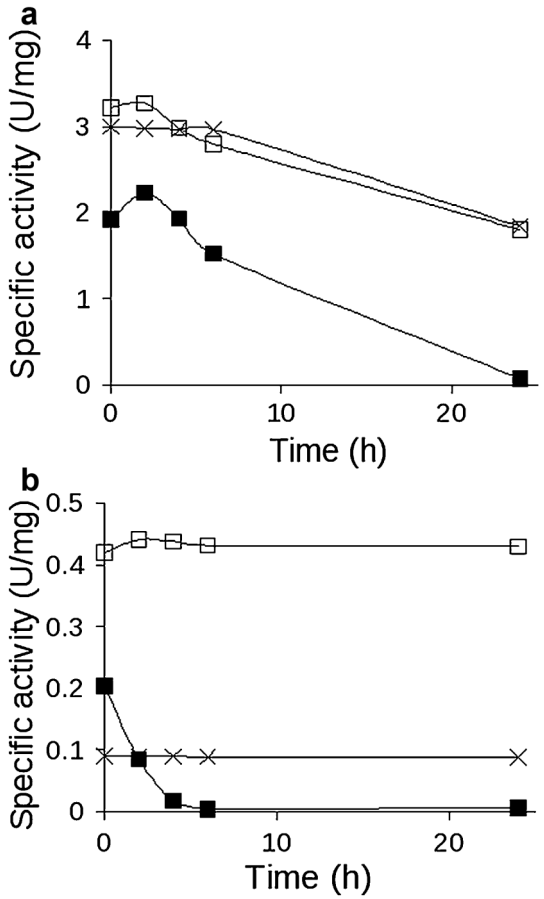

Figure 2. Stability of CHMO (**a**) with 0% (×), 1% (□), and 5% (■) MeOH and of PAMO (**b**) with 0% (×), 20% (□), and 40% (■) MeOH. Standard deviations were less than 10%.

In the other organic solvents, the residual activity of PAMO after 24 h was 35%, 1%, 13%, and 69% in 20% EtOH, 10% 1,1,1-trifluoroethanol (TFE), 10% acetonitrile (ACN), and 5% 1,4 dioxane, respectively. In the same organic solvents very little activity or no activity was observed in the case of CHMO.

Fluorescence Measurements

The fluorescence spectra of CHMO and PAMO were obtained at different MeOH concentrations and compared to those obtained with the standard N-Ac-Trp-OEt (Fig. S1a–c). The excitation wavelength was 295 nm in order to minimize the contribution of tyrosine fluorescence. Furthermore, the presence of 11 and 12 Trp residues in PAMO and CHMO, respectively, suggests that the fluorescence signals mostly arise from Trp residues. Nevertheless, on the basis of the current data, it was not possible to establish which residues were mostly involved in the generation of the observed fluorescence, although the similarity of the λ_{max} of emission (340 and 339 nm for CHMO and PAMO, respectively) and of Parameter A defined as IF_{320}/IF_{365} (in aqueous buffer was 1.0 for CHMO and 1.1 for PAMO; Fig. S1b,c) suggests that the fluorescence signals for the two enzymes come from Trp residues that have a similar surrounding. In fact, in the two enzymes most the Trp residues (9 out of 11/12) are conserved in the protein scaffold.

As an indication of the effect of the solvent on Trp fluorescence, spectra of the standard N-Ac-Trp-OEt were recorded at different percentages of MeOH. Increasing the concentration of MeOH from 0% to 50%, λ_{max} of emission showed a blue shift from 360 to 355 nm and a 1.5-fold increase of emission intensity from 95 to 147 a.u. (Fig. S1a). Such spectral variations are typically observed when the medium that surrounds the fluorophore becomes less polar. In particular, the 1.5-fold increase of fluorescence intensity at 50% MeOH is consistent with that reported by Muinő and Callis (1.3-fold, 2009).

The fluorescence spectral changes caused by MeOH for the two enzymes were different from that of the standard. In the case of CHMO, the increase of MeOH from 0% to 50% (v/v) produced a gradual red shift of the λ_{max} of emission (340–345 nm) and an increase of intensity of the fluorescence signal (Fig. S1b). In the case of PAMO a red shift from 339 to 344 nm and an increase of intensity was observed only for concentrations of MeOH higher than 20% (Fig. 3c). Therefore, on the basis of the variations of the λ_{max} of emission, the presence of MeOH causes a relatively more

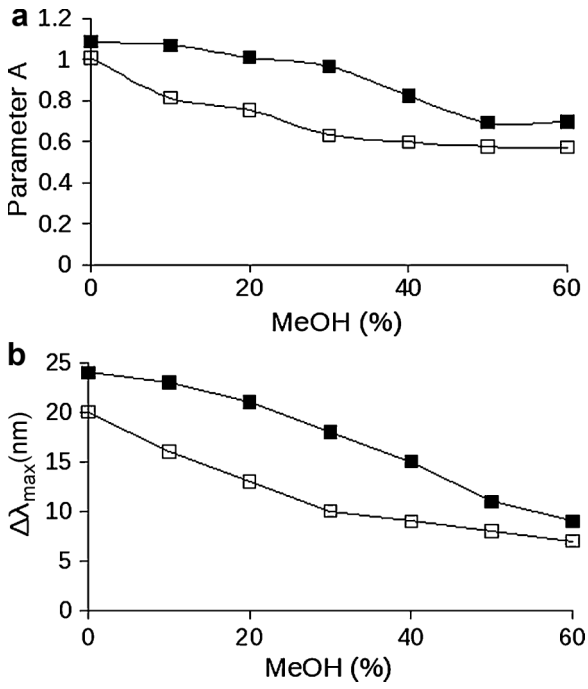

Figure 3. Variation of fluorescence spectra of CHMO (□) and PAMO (■) as a function of MeOH concentration monitored as parameter A [i.e., equal to the ratio of the spectral intensity at 320 nm over that at 365 nm (IF_{320}/IF_{365})] (**a**) or $\Delta\lambda_{max}$ of emission (**b**). Excitation wavelength 295 nm.

polar environment around the Trp residues responsible of the fluorescence spectrum, for both enzymes. This can be due to protein conformational changes that move the Trp residues from the hydrophobic core toward the protein surface and to the solvent. Because of this, the fluorescence signal could be less quenched explaining the increase of intensity.

A better correlation between fluorescence spectra and conformational changes can be deduced by plotting Parameter A and $\Delta\lambda_{max}$ of emission as a function of concentration of MeOH (Fig. 3a,b). $\Delta\lambda_{max}$ is the difference between λ_{max} of emission of the standard N-Ac-Trp-O-Et and λ_{max} of the protein. The use of $\Delta\lambda_{max}$ helps to distinguish the variations of fluorescence due to the Trp residues (partially) exposed on the protein surface (not necessarily due to protein conformational changes) from those due to the Trp residues in the protein core (Kijima et al., 1996). Therefore, a decrease of the $\Delta\lambda_{max}$ upon increase of the percentage of organic solvent points out a loss of tertiary structure (e.g., in the extreme case in which $\Delta\lambda_{max}$ is 0, the protein exposes all the Trp residues to the solvent because of complete unfolding). On the other hand, Parameter A, being the ratio of two points of the spectra, indicates if there are spectral variations independently of the position of the peak. For example, if two different conformational states are responsible for two different spectra, this could not be noted if only λ_{max} of emission is taken into consideration (Turoverov et al., 2002). Therefore, since both $\Delta\lambda_{max}$ and Parameter A vary as a function of MeOH concentration, it can be deduced that the organic solvent causes conformational changes in both CHMO and PAMO. However, the steeper decrease of Parameter A and of $\Delta\lambda_{max}$ of emission (as deducted by comparing $\Delta\Delta\lambda_{max}$ and ΔParameter A in Fig. S2 in Supplemental Materials) observed for CHMO indicates that this enzyme is more susceptible than PAMO to conformational changes caused by the addition of organic solvents. This also explains the lower C_{50} value observed for CHMO compared to PAMO (Table I).

The fluorescence data shown in Figure S1 also indicate that the fivefold enhancement of catalytic activity observed in the case of PAMO with 20% MeOH is not correlated to a major variation of the enzyme conformation (e.g., tertiary structure). In fact, at this concentration of MeOH, the spectrum of PAMO is very similar to that in buffer alone. Nevertheless, this does not rule out the possibility that minor conformational changes occurred and contribute to the enhancement of catalytic activity of PAMO.

Because BVMOs contain a tightly bound FAD cofactor, we investigated in more details the fluorescent properties of this flavin cofactor in the case of PAMO (Fig. 4). The fluorescence spectra of PAMO obtained by excitation at 440 nm strongly depended on the MeOH concentration (Fig. 4a). From buffer alone to 30% MeOH, a modest increase of intensity (about fourfold) was observed, but about a 70-fold increase of intensity was observed from 30% to 50% MeOH. Furthermore, passing from only buffer to

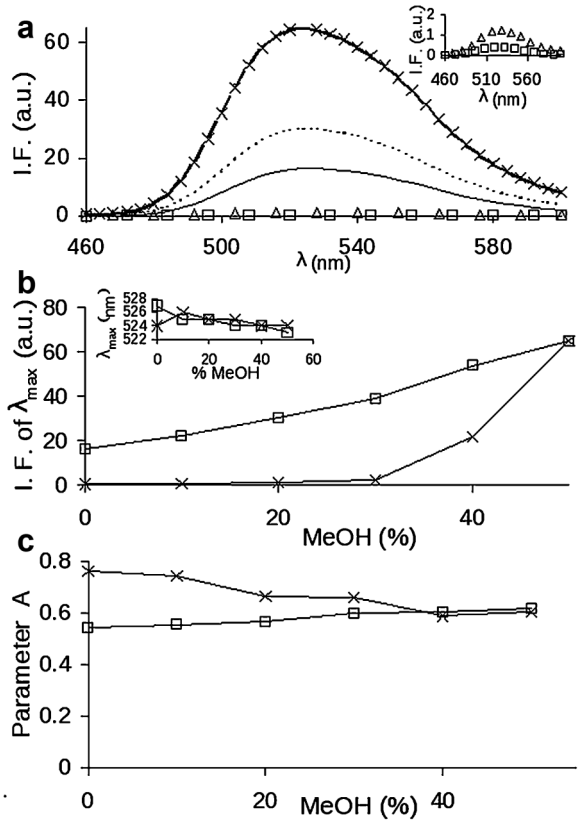

Figure 4. **a**: Fluorescence spectra of PAMO (symbols) and free FAD (lines) at 0% (□, thin), 20% (△, dashed), and 60% (×, thick) MeOH. Excitation wavelength 440 nm. In inset, expanded spectra of PAMO at 0% and 20% MeOH. **b**: Intensity of fluorescence and variation of the λ_{max} of emission (in inset) or (**c**) Parameter A of PAMO (x) and free FAD (□) as a function of MeOH concentration. Same symbols were used for PAMO and FAD in (b) and (c). Parameter A was obtained as ratio of fluorescence intensities emitted at 500 nm over that at 540 nm (IF_{500}/IF_{540}) of spectra reported in (a). Standard deviations were less than 10%. Spectra were not recorded at concentration higher than 60% MeOH because the enzyme solution were opalescent, suggesting protein precipitation.

10% MeOH, λ_{max} of emission varied from 524 to 526 nm and then it decreased to 524 nm at 50% MeOH (inset Fig. 4b). When the fluorescence of free FAD was investigated in buffer alone, FAD showed λ_{max} of emission at 527 nm and this value was 524 in the presence of 50% MeOH. Only a modest (fourfold) increase of fluorescence intensity was observed for free FAD when going from 0% to 50% MeOH. The much higher intensity of free FAD compared to that of FAD in PAMO indicates that in PAMO the flavin fluorescence is highly quenched as is common in flavoproteins (Fig. 4b). These results also agree with the crystallographic data which shows that the isoalloxazine ring of FAD in PAMO is only partially accessible to the solvent (Malito et al. 2004). In fact, we also observed that FAD fluorescence of PAMO is only weakly dependent on MeOH concentration up to 20%. Above this concentration, FAD fluorescence becomes strongly dependent on the solvent polarity, suggesting a higher accessibility of the solvent to the cofactor, likely due to protein unfolding. The same

conclusion was also drawn analyzing fluorescence data of FAD in terms of Parameter A (Fig. 4c). Indeed, the value of the Parameter A for free FAD and for FAD linked to PAMO converged toward the same value (about 0.65) as the concentration of MeOH increased, which agrees with a complete exposure to the solvent of the enzyme cofactor as consequence of major conformational changes and cofactor dissociation.

Circular Dichroism

With CD measurements, the secondary structure of a protein can be monitored. The signal due to α-helices (minima at around 220 and at 208 nm) prevails in the far-UV CD spectra of CHMO and PAMO recorded in buffer (Fig. 5a,b). Interestingly, the addition of MeOH causes a modest, in terms of intensity, but significant, in terms of form, variation of the CD spectra for the two enzymes. In the case of CHMO, passing from buffer alone to 20% MeOH, the CD spectrum is slightly modified undergoing a shift of the minimum (with increase of its intensity) from 210 to 208 nm and a concomitant 20% decrease of the intensity at 222 nm (near one of the two α-helix negative peaks). In the case of PAMO, at 20% MeOH the spectrum shows only a slight increase in intensity (especially at 208 nm, without any peak shift) with respect to that in buffer alone, suggesting that at this concentration of MeOH it preserves (or even slightly increases) the α-helix content. Similar increments have also been reported by other research groups with cytochrome *c* in the presence of methanol and ascribed to an increment of the protein helicity (Bychkova et al., 1996). At 50% MeOH, both CHMO and PAMO show a similar spectrum with a minimum at 214 nm, which indicates the loss of α-helical structures. However, in order to highlight the spectral variations the ratio of the intensity of the CD signal at 208 over that at 217 nm of CHMO and PAMO as a function of MeOH concentration was also compared (Fig. 6). This ratio can be taken as an indicator that emphasizes CD spectral variations and the trend of the ratio between α-helix and β-sheets. Calculation methods available online (e.g., DICHROWEB), useful for an estimation of the secondary structure from the CD spectra, were also taken into consideration (Whitmore and Wallace, 2004). However, although for PAMO in buffer, the calculated secondary structure (33% α-helix and 15% β-sheets) was in agreement with that found by X-ray analysis (35% α-helix and 17% β-sheets), for the CD spectra in the presence of MeOH (i.e., 20%), no variations of the secondary structure was shown by the calculation methods. This might indicate a "lower-sensitivity" of this approach to monitor spectral (and conformational) changes for this enzyme, with respect to the ratio of the intensities of peak-points of the CD spectrum. Therefore, we preferred to compare the effects of the organic solvent on the secondary structure for the two monooxygenases by the $\theta_{208}/\theta_{217}$ ratios. It should be emphasized that PAMO

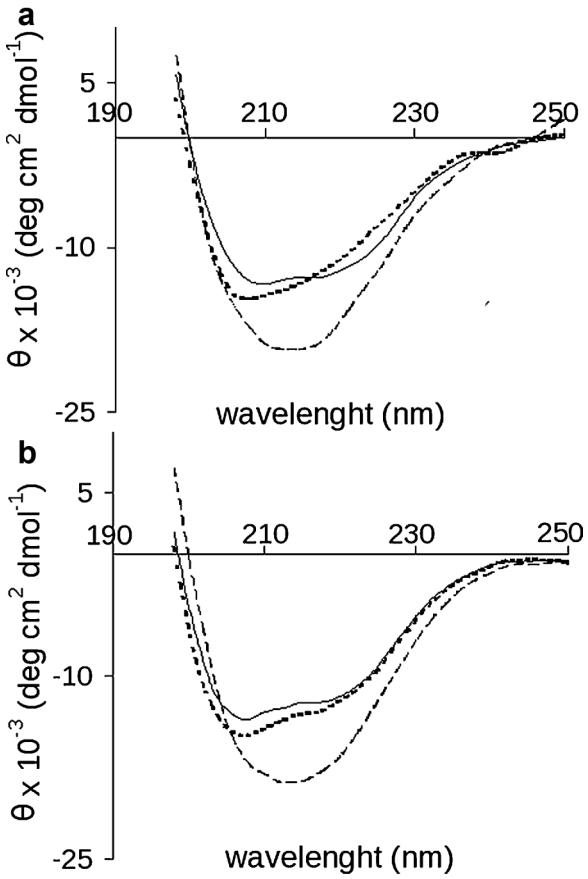

Figure 5. Circular dichroism spectra of CHMO (**a**) and PAMO (**b**) in buffer (thin), in the presence of 20% (thick and short dashes) and 50% (thin and long dashes) MeOH. Molar mean residue ellipticity (θ) were calculated from the equation: $\theta = \theta_{obs} \times MW_m / 10 \times d \times c$ where θ_{obs} is the ellipticity measured in degrees, MW_m is the mean residue molar weight of the enzyme (110.7 g/mol for CHMO and 118.5 g/mol for PAMO), *c* is the protein concentration (0.12 g/mL), and *d* is the optical path (0.1 cm).

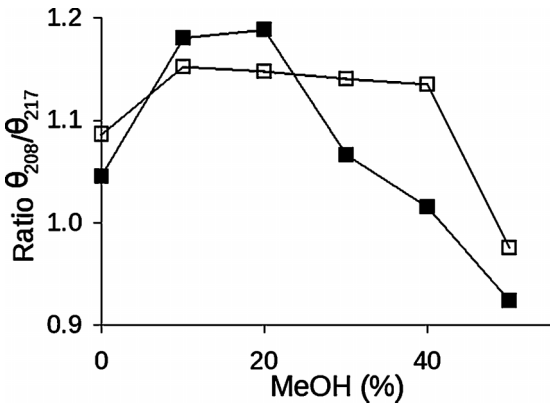

Figure 6. Variation of CD spectra of CHMO (■) and PAMO (□) as a function of MeOH concentration monitored as $\theta_{208}/\theta_{217}$ ratio. Standard deviations were less than 10%.

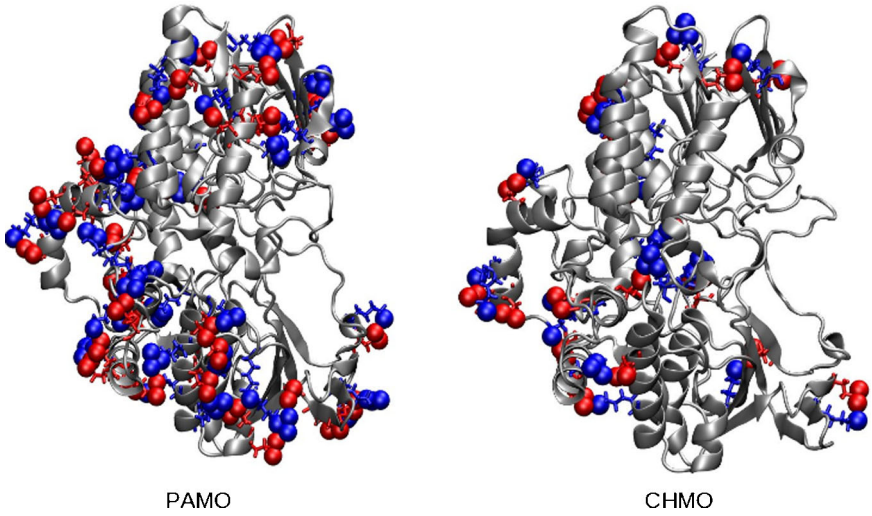

Figure 7. Representation of the structure of PAMO (**left**) and CHMO (**right**). Positively charged residues are shown in blue and negatively charged residues are shown in red. [Color figure can be seen in the online version of this article, available at wileyonlinelibrary.com.]

undergoes only a small variation of the $\theta_{208}/\theta_{217}$ ratios at about 10% MeOH and then remains similar up to 40% MeOH, where it plunges. Instead, for CHMO the same ratio drastically decreases starting from 20% MeOH. These results suggest a less stable secondary structure in CHMO than in PAMO.

Computational Comparison of the Structures of PAMO and CHMO

In order to shed light on the molecular reasons that determine a different conformational stability of the two enzymes toward organic solvent, we compared the structures of PAMO and CHMO. The sequence identity of the CHMO from *Acinetobacter calcoaceticus* and cyclohexanone monooxygenase from *Rhodococcus* sp. strain HI-31 (540 amino acids) is 57%. This allowed the elaboration by homology modeling of a sufficiently representative CHMO structure, for which no 3D structure is available (Fig. 7).

A possible reason for the enhanced stability of PAMO versus CHMO from a structural viewpoint might be related to the fact that PAMO appears to have a higher number of salt bridges than CHMO. In fact, PAMO has 41 salt bridges, whereas the homology model of CHMO from *Acinetobacter* shows 31 or 20 salt bridges when the model was obtained from the closed (3GWD) or the open (3GWF) structure of cyclohexanone monooxygenase from *Rhodococcus* sp., respectively. It is worthwhile to emphasize that the number of salt bridges found in the homology models of PAMO obtained from the two crystals structure of cyclohexanone monooxygenase from *Rhodococcus* sp. were 33 (with 3GWD) and 24 (with 3GWF), which also confirms the higher number of salt bridges in PAMO compared to CHMO from *Acinetobacter*. The salt bridges in PAMO are well distributed all over the structure and work like a belt around the structure, increasing the stability of this enzyme in water–organic solvent mixtures (Gong and Freed, 2010; Fig. 7). The higher number of hydrogen bonds in PAMO compared to CHMO (529 and 440, respectively) can also contribute to the increased stability. In contrast, we excluded the possibility that the percentage of internal hydrophobic residues substantially contribute to the different stability because they were similar in the two enzymes (44% in PAMO and 49% in CHMO).

Conclusions

Fluorescence and CD data demonstrated that the decrease of catalytic activity for PAMO and CHMO as a function of the concentration of organic solvents in the medium can be mainly ascribed to a loss of tertiary and secondary structures. However, the study herein presented showed that PAMO has a higher stability than CHMO toward organic solvents. It was also shown that 20% MeOH (v/v) can highly enhance the activity of PAMO. In spite of the fact that no major conformational changes of PAMO were observed at 20% MeOH, it cannot be excluded that small conformational changes in the whole enzyme (e.g., increase of protein helicity) or in the active site play an important role in enzyme activity. It was already noted for PAMO that the enzyme can be activated by prolonged incubations at relatively high temperature which suggests that the enzyme can indeed adopt a slightly different and more active conformation (Fraaije et al., 2005). Similar subtle structural changes have been linked with thermal activation of thermostable enzymes (Klump et al. 1992). Above 20% MeOH, the unfolding of PAMO is more pronounced,

resulting in the disruption of the catalytic system. This process occurs at lower concentration of organic solvents in the case of CHMO. It is worth noting that CHMO has a higher specific activity than PAMO with thioanisole. Therefore, it appears that PAMO has to be ''loosened'' to better accommodate and/or transform this substrate. To this end, it has to be noted that the presence of MeOH causes a decrease of thermal stability of PAMO. In fact T_m, measured by plotting Parameter A of the fluorescence spectra recorded as a function of temperature, passed from about 54°C in buffer alone to 44°C with 20% MeOH (Fig. S3), which indicates that the organic solvent makes protein structure less rigid and more prone to unfolding. Furthermore, this study highlights that salt bridges, which are known to increase the protein thermal stability, also increase the stability of enzymes in water–organic solvent mixtures.

We thank Donatella Varinelli for skillful technical assistance.

References

Abagyan RA, Totrov MM. 1994. Biased probability Monte Carlo conformational searches and electrostatic calculations for peptides and proteins. J Mol Biol 235:983–1002.

Alphand V, Carrea G, Wohlgemuth R, Furstoss R, Woodley JM. 2003. Towards large-scale synthetic applications of Baeyer–Villiger monooxygenases. Trends Biotechnol 21:318–323.

Bocola M, Schulz F, Leca F, Vogel A, Fraaije MW, Reetz MT. 2005. Converting phenylacetone monooxygenase into phenylcyclohexanone monooxygenase by rational design: Towards practical Baeyer–Villiger monooxygenases. Adv Synth Catal 347:979–986.

Bychkova VE, Dujsekina AE, Klenin SI, Tiktopulo EI, Uversky VN, Ptitsyn OB. 1996. Molten globule-like state of cytochrome c under conditions simulating those near the membrane surface. Biochemistry 35:6058–6063.

Colonna S, Gaggero N, Pasta P, Ottolina G. 1996. Enantioselective oxidation of sulfides to sulfoxides catalyzed by bacterial cyclohexanone monooxygenases. Chem Commun 20:2303–2307.

De Gonzalo G, Ottolina G, Zambianchi F, Fraaije MW, Carrea G. 2006. Biocatalytic properties of Baeyer–Villiger monooxygenases in aqueous-organic media. J Mol Catal B-Enzym 39:91–97.

Donoghue NA, Norris DB, Trudgill PW. 1976. The purification and properties of cyclohexanone oxygenase from *Nocardia globerula* CL1 and *Acinetobacter* NCIB 9871. Eur J Biochem 63:175–192.

Fraaije MW, Wu J, Heuts DPHM, van Hellemond EW, Spelberg JHL, Janssen DB. 2005. Discovery of a thermostable Baeyer–Villiger monooxygenase by genome mining. Appl Microbiol Biotechnol 66:393–400.

Gong H, Freed KF. 2010. Electrostatic solvation energy for two oppositely charged ions in a solvated protein system: Salt bridges can stabilize proteins. Biophys J 98:470–477.

Gupta MN, Batra R, Tyagi R, Sharma A. 1997. Polarity index: The guiding solvent parameter for enzyme stability in aqueous–organic cosolvent mixture. Biotechnol Progr 13:284–288.

Humphrey W, Dalke A, Schulten K. 1996. VMD: Visual molecular dynamics. J Mol Graph 14:33–38.

Kamerbeek NM, Janssen DB, Berkel WJH, van Fraaije MW. 2003. Baeyer–Villiger monooxygenases, an emerging family of flavin-dependent biocatalysts. Adv Synth Catal 345:1–12.

Kayser MM. 2009. ''Designer reagents'' recombinant microorganisms: New and powerful tools for organic synthesis. Tetrahedron 65:947–974.

Khmelnitsky YL, Mozhaev VV, Belova AB, Sergeeva MV, Martinek K. 1991. Denaturation capacity: A new quantitative criterion for selection of organic solvents as reaction media in biocatalysis. Eur J Biochem 198:31–41.

Kijima T, Yamamoto S, Kise H. 1996. Study on tryptophan fluorescence and catalytic activity of alpha-chymotrypsin in aqueous-organic media. Enzyme Microb Tech 18:2–6.

Klump H, Di Ruggiero J, Kessel M, Park JB, Adams MW, Robb FT. 1992. Glutamate dehydrogenase from the hyperthermophile *Pyrococcus furiosus*. Thermal denaturation and activation. J Biol Chem 267:22681–22685.

Kudryashova EV, Artemova TM, Vinogradov AA, Gladilin AK, Mozhaev VV, Levashov AV. 2003. Stabilization and activation of α-chymotrypsin in water–organic solvent systems by complex formation with oligoamines. Protein Eng 16:303–309.

Leo A, Hansch C, Elkins D. 1971. Partition coefficients and their uses. Chem Rev 71:525–616.

Malito E, Alfieri A, Fraaije MW, Mattevi A. 2004. Crystal structure of a Baeyer–Villiger monooxygenase. Proc Natl Acad Sci USA 101:13157–13162.

Mihovilovic MD. 2006. Enzyme mediated Baeyer–Villiger oxidations. Curr Org Chem 10:1265–1287.

Mirza IA, Yachnin BJ, Wang S, Grosse S, Bergeron H, Imura A, Iwaki H, Hasegawa Y, Lau PC, Berghuis AM. 2009. Crystal structures of cyclohexanone monooxygenase reveal complex domain movements and a sliding cofactor. J Am Chem Soc 131:8848–8854.

Muinő PL, Callis PR. 2009. Solvent effects on the fluorescence quenching of tryptophan by amides via electron transfer. Experimental and computational studies. J Phys Chem B 113:2572–2577.

Ogino H, Gemba Y, Yamada M, Shizuka M, Yasuda M, Ishikawa H. 2000. The synthetic rate of dipeptide catalyzed by organic solvent-stable protease from *Pseudomonas aeruginosa* PST-01 in the presence of water-soluble organic solvents. Biochem Eng J 5:219–223.

Olofsson L, Nicholls IA, Wikman S. 2005. TBADH activity in water-miscible organic solvents: Correlations between enzyme performance, enantioselectivity and protein structure through spectroscopic studies. Org Biomol Chem 3:750–755.

Olofsson L, Nicholls IA, Söderberg P. 2006. Influence of water miscible organic solvents on α-chymotrypsin in solution and immobilized on Eupergit CM. Biotechnol Lett 28:929–935.

Ottolina G, Bianchi S, Belloni B, Carrea G, Danieli B. 1999. First asymmetric oxidation of tertiary amines by cyclohexanone monooxygenase. Tetrahedron Lett 40:8483–8486.

Öztürk DC, Kazan D, Denizci AA, Grimoldi D, Secundo F, Erarslan A. 2010. Water miscible mono alcohols effect on the structural conformation of *Bacillus clausii* GMBAE 42 serine alkaline protease. J Mol Catal B-Enzym 64:184–188.

Park H, Lee KS, Chi YM, Jeong SW. 2005. Effects of methanol on the catalytic properties of porcine pancreatic lipase. J Microbiol Biotechnol 15:296–301.

Riddick JA, Bunger WB, Sakano TK. 1986. Organic solvents: Physical properties and methods of purification. In: Weissberger A, editor. Techniques of Chemistry, Vol. 2. pp 191, 193, 700. 4th edition. New York: Wiley.

Secundo F, Zambianchi F, Crippa G, Carrea G, Tedeschi G. 2005. Comparative study of the properties of wild type and recombinant cyclohexanone monooxygenase, an enzyme of synthetic interest. J Mol Catal B-Enzym 34:1–6.

Sheng DW, Ballou DP, Massey V. 2001. Mechanistic studies of cyclohexanone monooxygenase: Chemical properties of intermediates involved in catalysis. Biochemistry 40:11156–11167.

Tan KH, Lovrien R. 1972. Enzymology in aqueous–organic cosolvent binary mixtures. J Biol Chem 247:3278–3285.

Torres Pazmiño DE, Baas BJ, Janssen DB, Fraaije MW. 2008. Kinetic mechanism of phenylacetone monooxygenase from *Thermobifida fusca*. Biochemistry 47:4082–4093.

Torres Pazmiño DE, Dudek HM, Fraaije MW. 2010. Baeyer–Villiger monooxygenases: Recent advances and future challenges. Curr Opin Chem Biol 14:138–144.

Tóth K, Sedlák E, Musatov A, Žoldák G. 2010. Activity of NADH oxidase from *Thermus thermophilus* in water/alcohol binary mixtures is limited by the stability of quaternary structure. J Mol Catal B-Enzym 64: 60–67.

Turoverov KK, Verkhusha VV, Shavlovsky MM, Biktashev AG, Povarova OI, Kuznetsova IM. 2002. Kinetics of actin unfolding induced by guanidine hydrochloride. Biochemistry 41:1014–1019.

Weiner SJ, Kollman PA, Case DA, Singh UC, Ghio C, Alagona G, Profeta S, Weiner PJ. 1984. A new force field for molecular mechanical simulation of nucleic acids and proteins. J Am Chem Soc 106:765–784.

Weiner SJ, Kollman PA, Nguyen DT, Case DA. 1986. An all atom force field for simulations of proteins and nucleic acids. J Comput Chem 7:230–252.

Whitmore L, Wallace BA. 2004. DICHROWEB, an online server for protein secondary structure analyses from circular dichroism spectroscopic data. Nucleic Acids Res 32:W668–W673.

Willetts A. 1997. Structural studies and synthetic applications of Baeyer–Villiger monooxygenases. Trends Biotechnol 15:55–62.

Woodley JM. 2008. New opportunities for biocatalysis: Making pharmaceutical processes greener. Trends Biotechnol 26:321–327.